

Generalizable Synthetic Image Detection via Language-guided Contrastive Learning

Haiwei Wu Jiantao Zhou* Shile Zhang
State Key Laboratory of Internet of Things for Smart City
Department of Computer and Information Science
University of Macau, Macau, People’s Republic of China
{yc07912, jtzhou, mc14950}@um.edu.mo

Abstract

The heightened realism of AI-generated images can be attributed to the rapid development of synthetic models, including generative adversarial networks (GANs) and diffusion models (DMs). The malevolent use of synthetic images, such as the dissemination of fake news or the creation of fake profiles, however, raises significant concerns regarding the authenticity of images. Though many forensic algorithms have been developed for detecting synthetic images, their performance, especially the generalization capability, is still far from being adequate to cope with the increasing number of synthetic models. In this work, we propose a simple yet very effective synthetic image detection method via a language-guided contrastive learning and a new formulation of the detection problem. We first augment the training images with carefully-designed textual labels, enabling us to use a joint image-text contrastive learning for the forensic feature extraction. In addition, we formulate the synthetic image detection as an identification problem, which is vastly different from the traditional classification-based approaches. It is shown that our proposed LanguAge-guided SynThEsis Detection (LASTED) model achieves much improved generalizability to unseen image generation models and delivers promising performance that far exceeds state-of-the-art competitors by +22.66% accuracy and +15.24% AUC. The code is available at <https://github.com/HighwayWu/LASTED>.

1. Introduction

The unyielding progress of deep learning has given rise to numerous prominent generative models, including generative adversarial networks (GANs) and diffusion models (DMs). The photorealism and creativity exhibited by the images synthesized through these models have received increasing attention from various communities. In August of

2022, a DM-generated painting named Theater d’Opera Spatial claimed the first prize at the Colorado State Fair’s digital art competition, catapulting generative models into the spotlight. While generative models may serve as a source of inspiration for artists and designers or provide entertainment, there is a grave apprehension regarding their potential for malicious use in the generation and dissemination of misinformation. Under this circumstance, it is urgent to develop forensic algorithms, capable of distinguishing synthetic images from real ones.

Several algorithms [18, 23, 40, 76] have been put forth to detect synthetic images by examining distinct artifacts left behind in the generation process. Along this line, Zhang *et al.* [81] introduced a spectrum-based method that detects checkerboard artifacts produced by GANs, which tend to form spectra replications in the frequency domain. Chandrasegaran *et al.* [18] claimed that the color information is a critical forensic feature for detecting GAN-generated images, as GANs struggle to capture the color distribution of underlying images. Wang *et al.* [76] proposed a data augmentation strategy, including compression and blurring, to enhance the detector’s generalization capability. Recently, Corvi *et al.* [23] initiated the research on detecting DM-generated images, revealing that detectors trained solely on GAN images have inadequate generalizability to detect DM images. Despite the relative success of these algorithms, their performance, especially the generalization capability, is still far from being adequate to cope with the increasing number of synthetic models.

In this work, we aim to enhance the generalizability of the synthetic image detector by rethinking two key aspects: training paradigm and testing procedure. From the perspective of training, a large body of works [43, 44, 65, 73] (and references therein) have shown that contrastive learning can enhance the general representation ability of neural networks. In particular, CLIP [65], which is based on language supervision and contrastive paradigm, can even compete

*Corresponding author.

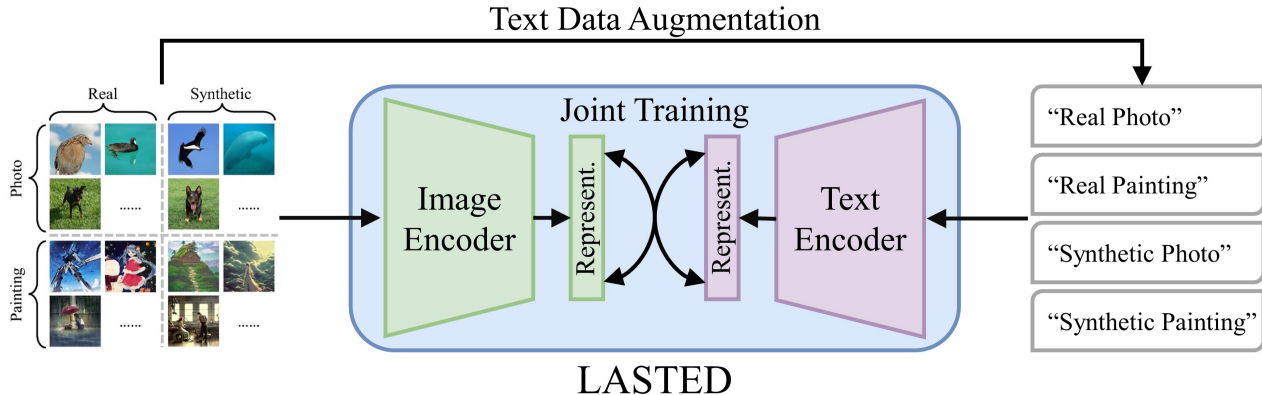


Figure 1. Illustration of our proposed LASTED. The training images are first augmented with the carefully-designed textual labels, and then image/text encoders are jointly trained.

with supervised training models in many tasks. Inspired by this, we propose a new synthetic image detection method: LanguAge-guided SynThEsis Detection (LASTED), which utilizes an augmented language supervision to improve the image-domain forensic feature extraction. Noticing that the training data (synthetic or real images) usually do not accompany with textual information, we propose to augment them with carefully-designed textual labels: “Real Photo”, “Real Painting”, “Synthetic Photo”, and “Synthetic Painting”. Upon having the image-text pairs, our LASTED jointly trains an image encoder and a text encoder to predict the matched pairings of a batch of (image, text) examples under a contrastive learning framework. Essentially, the augmented textual labels provide learnable high-dimensional targets, which do not have to be composed of orthogonal one-hot vectors, thus making the semantic decoupling of “Real Photo”, “Real Painting”, “Synthetic Photo”, and “Synthetic Painting” easier to be optimized. The training process of our LASTED is illustrated in Fig. 1.

On the other hand, from the perspective of testing procedure, we propose to formulate synthetic image detection as an identification problem, which is vastly different from the existing classification-based approaches. To be more specific, our goal now becomes to determine whether a given set of images belong to the same category (real or synthetic), rather than predicting which specific category they are from. This is a bit analogous to face recognition [28, 59, 73] and camera model recognition [25, 56, 58] problems, where we only need to determine whether given images belong to the same ID or camera. Formulating such an identification task for the synthetic image detection allows us to extract highly discriminative representations from limited data, thereby enhancing the detector’s capability to generalize against distributional inconsistencies between training and testing datasets. To fit the identification task, our proposed LASTED abandons the final linear classifier used in [18, 40, 76], and changes the optimization objective from predicting fixed set

of category logits to extracting highly discriminative features for the synthetic image detection.

It is shown that our proposed LASTED model achieves much improved generalizability to unseen image generation models and delivers promising performance that far exceeds state-of-the-art competitors [18, 40, 76] by +22.66% accuracy and +15.24% AUC. In summary, this work presents the following significant contributions:

- By incorporating carefully-designed textual labels, we devise LASTED for detecting synthetic images based on language supervision, capable of extracting highly discriminative features from the joint image-text space under a contrastive learning framework.
- We propose to formulate the synthetic image detection as an identification (rather than classification) problem, which is more equipped to tackle distributional inconsistencies between training and testing datasets.
- Experimental results demonstrate the superiority of the proposed LASTED over state-of-the-art methods, with a significant improvement of +22.66% accuracy and +15.24% AUC.

The rest of this paper covers the following contents. Section 2 reviews the related works on detecting synthetic images. Section 3 presents our proposed LASTED. Experimental results are given in Section 4 and Section 5 summarizes.

2. Related Works on Synthetic Image Detection

In recent years, many detection algorithms [17, 18, 24, 33–35, 37–39, 46–48, 57, 61, 70, 76, 80, 81] have been proposed to combat the potential malicious use of AI-generated images. Typically, these algorithms leverage the unique traces left by the image synthesis process, such as checkerboard artifacts [61] in the pixel-domain. Through frequency-domain analysis, Dzanic *et al.* [34] and Durall *et al.* [33] showed

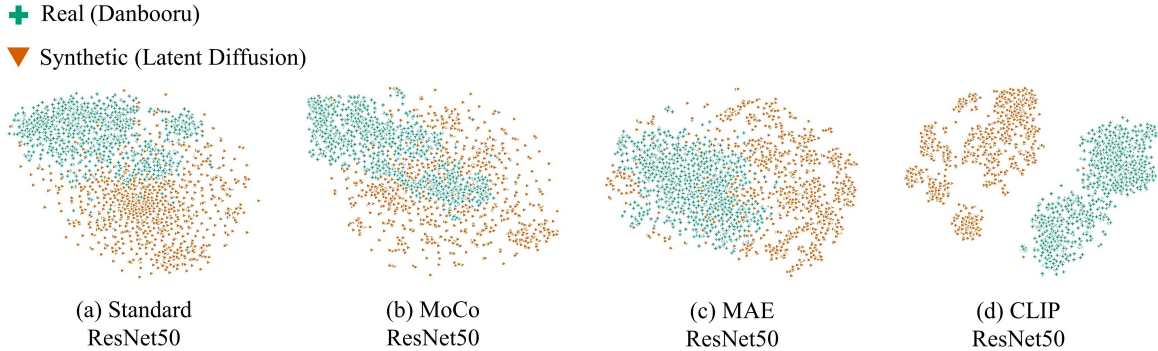


Figure 2. Different training paradigms (MoCo [44], MAE [43], and CLIP [65]) lead to different generalizability. It is worth noting that all models use the same ResNet50 [45] architecture and are trained on a natural image dataset (*e.g.*, ImageNet [27]) without fine-tuning. The testing is carried out on unseen real painting images (Danbooru [3]) and the ones synthesized by Latent Diffusion [69].

that GAN-generated images deviate from real data in terms of spectral distribution. In this regard, some studies [37, 81] suggested spectrum-based detection techniques and demonstrated their effectiveness. In addition, Wang *et al.* [76] developed a detector with stronger generalizability by devising a well-crafted data augmentation strategy, so as to detect unknown GAN-generated images. Moreover, Chandrasegaran *et al.* [18] posited that color information is an important forensic feature with good transferability, which can be exploited to facilitate the synthetic image detection. Recently, Corvi *et al.* [23] disclosed that detectors trained only on GAN-generated images cannot generalize well to detect DM-generated ones. Their results indicate that DM images are characterized by distinct artifacts from those of GAN images.

3. LASTED for Synthetic Image Detection

Our goal is to design a synthetic image detector, termed LASTED, that can generalize well to unseen data. This is achieved by improving the training paradigm with the assistance of language supervision and by formulating the synthetic image detection in the testing phase as an identification problem. In the following, we first introduce the motivation of utilizing augmented language supervision, followed by the details on how to design the textual labels. Eventually, the detailed training and testing procedures of our LASTED are given.

3.1. Motivation

The training paradigm based on contrastive learning has been proven to have strong generalizability and zero-shot transferability in the field of image classification [27, 43, 44, 65]. Inspired by this, we attempt to involve the contrastive learning in the task of synthetic image detection. To explore which contrastive paradigm is most suitable, we evaluate three famous paradigms, namely, MoCo [44], MAE [43], and CLIP [65], on their abilities to extract generalizable

Choice	Textual Labels
\mathcal{R}_1	“Real”, “Synthetic”
\mathcal{R}_2	“Real Photo”, “Real Painting”, “Synthetic Photo”, “Synthetic Painting”
\mathcal{R}_3	“Photo Real”, “Painting Real”, “Photo Synthetic”, “Painting Synthetic”
\mathcal{R}_4	“Real-Photo”, “Real-Painting”, “Synthetic-Photo”, “Synthetic-Painting”
\mathcal{R}_5	“A B”, “A C”, “D B”, “D C”

Table 1. Different textual labeling strategies.

representations for discriminating unseen real (Danbooru [3]) and synthetic (Latent Diffusion [69]) painting images. The extracted features, visualized by T-SNE [29], are shown in Fig. 2. Note that no fine-tuning is conducted on these three models. It can be seen that although these models are only trained on real natural photos (*e.g.*, ImageNet [27]), they can still extract highly discriminative representations from real/synthetic painting images, which are unseen in the training phase. In particular, the representations extracted by CLIP can almost perfectly distinguish painting images from Danbooru and Latent Diffusion. We therefore speculate that although DM or GAN synthesized images have good visual realism, they can be still easily distinguishable in the joint visual-language feature space. This serves as our motivation of using language-guided contrastive training paradigm for the task of synthetic image detection.

3.2. Augmenting with Textual Labels

The first challenge for exploiting joint visual-language features is that the training images (real or synthetic) do not naturally accompany with textual information. It is hence crucial to design a text data augmentation strategy to specifically fit the synthetic image detection task. A naive method, to this end, is to manually associate a single word “Real” or “Synthetic” to each image in the training dataset (see \mathcal{R}_1 in Table 1), based on whether it is real or synthesized. However, we experimentally find that this simple labeling scheme leads to rather poor generalization in the synthetic image detection task. This is because there are different types of real (similarly synthetic) images, such as those captured by cameras (*e.g.*, ImageNet [27]) and the ones drawn by humans through

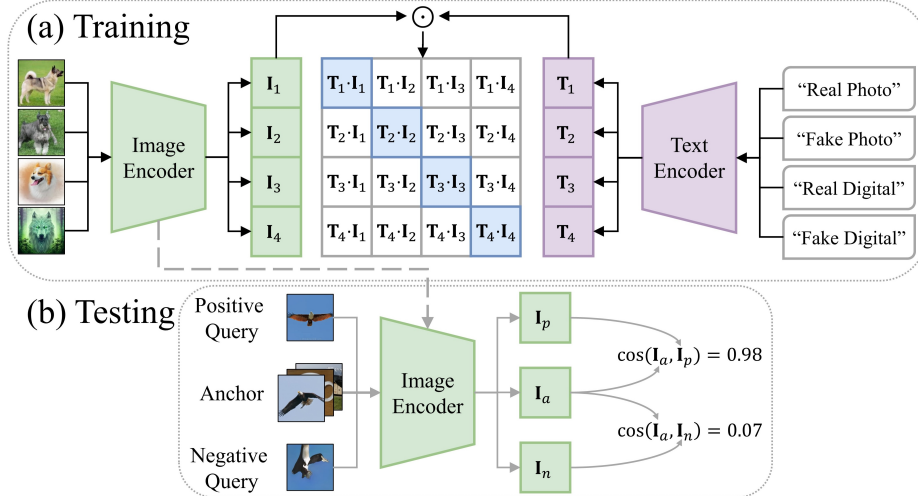


Figure 3. Our proposed LASTED framework. Noted that the text encoder is only used for supervising the training phase and will be discarded in the testing procedure.

Photoshop or digital plates (*e.g.*, Danbooru [3]). Clearly, these two types of real images have significantly different forensic features, *e.g.*, the presence of camera traces in real photos and fictional elements in painting images, and hence, should not be mixed into the same category with the same “Real” label. To solve this problem, we propose to append secondary labels “Photo” and “Painting” to distinguish the aforementioned two types of images. We hence define four labels “Real Photo”, “Real Painting”, “Synthetic Photo”, and “Synthetic Painting”¹, using which all training images are augmented with textual information. While it is possible to further append with more texts, such as “Indoor” and “Outdoor”, this would significantly increase the cost of labeling and the subsequent training.

Some alternative labeling strategies are given in Table 1. For instance, since textual labels are characters representing abstract concepts, their order can be disrupted (\mathcal{R}_3) or even substituted with simple alphabets (\mathcal{R}_5). An interesting variation is \mathcal{R}_4 , which, for instance, adds a hyphen to connect the “Real” and “Photo” labels to form “Real-Photo”. Although \mathcal{R}_4 is similar to \mathcal{R}_2 , it conveys a completely different meaning because “Real-Photo” no longer has any implicit association with “Real-Painting” and “Synthetic-Photo”. Ablation studies to be presented in Sec. 4.4 will show that \mathcal{R}_4 labeling choice results in a 6% decrease in the detection accuracy. Now, we are ready to introduce the training and testing processes of our LASTED.

¹“Real Photo” refers to natural images captured by any sort of camera, while “Real Painting” means digital images drawn by humans via digital tools. Also, “Synthetic Photo” and “Synthetic Painting” respectively represent the images synthesized using GAN or DM techniques, depending on whether photo or painting data are used for training. In this work, we do not consider those compound images, in which two or more of the above four types are mixed into an individual image.

3.3. Training Process of LASTED

The training procedure of our LASTED is depicted in Fig. 3 (a), which mainly involves two encoders, namely, the image encoder f_θ and the text encoder g_ϕ . Given a dataset consisting of N paired images and their augmented textual labels $\{(\mathbf{X}_i, \mathbf{Y}_i)\}_{i=1}^N$, the encoders first extract visual and textual representations $\mathbf{I}_i = f_\theta(\mathbf{X}_i)$ and $\mathbf{T}_i = g_\phi(\mathbf{Y}_i)$, respectively. Here, $\mathbf{Y}_i \in \mathcal{R}_2$, namely, \mathbf{Y}_i is one of the C predefined textual labels. The objective function is designed to maximize the cosine similarity of visual and textual representations of the matched pairings (see blue boxes in Fig. 3 (a)), while minimizing the unmatched pairings (see white boxes). Formally, the objective loss along the image axis can be expressed as:

$$\mathcal{L}_I = \frac{1}{N} \sum_{i=1}^N -\log \frac{\exp(\mathbf{I}_i \cdot \mathbf{T}_i / \tau)}{\sum_{j \in [1, C]} \exp(\mathbf{I}_i \cdot \mathbf{T}_j / \tau)}. \quad (1)$$

Similarly, we can calculate the loss along the text axis by:

$$\mathcal{L}_T = \frac{1}{C} \sum_{j=1}^C -\log \frac{\sum_{k \in [1, N], \mathbf{T}_k = \mathbf{T}_j} \exp(\mathbf{T}_k \cdot \mathbf{I}_k / \tau)}{\sum_{i \in [1, N]} \exp(\mathbf{T}_j \cdot \mathbf{I}_i / \tau)}, \quad (2)$$

where τ is a learned temperature parameter [65]. The overall loss then becomes $\mathcal{L} = \mathcal{L}_I + \mathcal{L}_T$.

Regarding the network architectures, we adopt ResNet50x64 [65] and Text Transformer [66] for the image encoder f_θ and text encoder g_ϕ , respectively. It should also be noted that the selection of networks is diverse, as long as the extracted representations \mathbf{I} and \mathbf{T} share the same dimensional feature space. The ablation studies on using different image encoders will be given in Sec. 4.4.

3.4. Testing Process of LASTED

Upon the training, the well-trained image encoder f_θ is then used in testing procedure as illustrated in Fig. 3 (b), while the text encoder g_ϕ is discarded. Since f_θ is designed to only extract image representations and cannot directly output specific category labels, we propose to use a small amount of data with the same label (denoted as anchor set) to assist in the testing procedure. In practice, it is rather simple to obtain the anchor sets by collecting images of the same category (such as “Real Photo”, “Real Painting”, etc). For instance, randomly sampling ImageNet [27] could result in an anchor set for “Real Photo”. Let $\mathcal{A} = \{\mathbf{A}_1, \mathbf{A}_2, \dots, \mathbf{A}_M\}$ be an anchor set with M images, and the representation of this anchor set can be computed by:

$$\mathbf{I}_a = \frac{1}{M} \sum_{m=1}^M \mathbf{I}_m \quad (3)$$

where \mathbf{I}_m denotes the representation of \mathbf{A}_m extracted by f_θ . In other words, the mean representation of all the images in the anchor set is adopted.

When an image under investigation with representation \mathbf{I}_q arrives, we determine whether it belongs to the same category as the anchor set by calculating its similarity score S with the anchor representation \mathbf{I}_a . Specifically, S is the cosine similarity between normalized \mathbf{I}_q and \mathbf{I}_a :

$$S(\mathbf{I}_q, \mathbf{I}_a) = \cos\left(\frac{\mathbf{I}_q}{\|\mathbf{I}_q\|}, \frac{\mathbf{I}_a}{\|\mathbf{I}_a\|}\right). \quad (4)$$

Clearly, images with the same category as the anchor set are expected to have a higher value of S (positive queries), and vice versa. To predict a hard label rather than soft score, a predefined threshold th is exploited for thresholding the cosine similarity S . For instance, th can be set as the median of S for investigated images, or simply as 0.5.

It is worth noting that in the aforementioned testing procedures, neither textual labels nor text encoder are necessary. However, if we have prior knowledge that the testing data share the same categories as the training data, the text encoder g_ϕ can also be employed to assist in determining the specific category of a given testing image, without requiring any anchor set. More specifically, the predicted label $\hat{\mathbf{Y}}_i$ can be computed as follows:

$$\hat{\mathbf{Y}}_i = \operatorname{argmax}_{\mathbf{Y}_i} S(\mathbf{I}_q, g_\phi(\mathbf{Y}_i)), \quad (5)$$

where \mathbf{Y}_i is the i th textual label.

In addition, given different anchor sets, LASTED can be applied for different applications such as image source identification, *i.e.*, determining whether an image is generated by a specific GAN or DM. Also, we can directly measure the probability of two given representations belonging to the same category, without using any anchor set, if the specific label information is not crucial.

4. Experiments

4.1. Settings

Training Dataset: We form the training dataset by including four categories of data, namely, real photos from LSUN [79], real paintings from Danbooru [3], synthetic photos by ProGAN [49], and synthetic paintings by Stable Diffusion (SD) [9, 11] from [6]. The image synthesis models ProGAN and SD here are deliberately trained on LSUN and Danbooru, respectively, forcing the detector to learn more discriminative representations from visually similar real and synthetic images. Each category contains 200K images, among which 1% images are split as validation data.

Testing Datasets: Two testing datasets are constructed for evaluating the performance of the synthetic image detection, namely, open-set dataset \mathcal{T}_{open} and practical dataset \mathcal{T}_{pra} . Specifically, \mathcal{T}_{open} adopts seven representative image synthesis models to generate cross-domain synthetic images, including three GANs (BigGAN [15], GauGAN [63], and StyleGAN [50]) and four DMs (DALLE [67], GLIDE [60], Guided Diffusion [30], and Latent Diffusion [69]). In addition, we randomly sample images from real photo datasets ImageNet [27] and VISION [71], and real painting datasets Danbooru [3] and Artist [1, 2], where the sampling is balanced among different datasets. Totally, we form 14 testing subsets, each of which contains 2K real (photo or painting) and 2K synthetic (GAN- or DM-generated) images. For instance, the first testing subset contains 1K ImageNet, 1K VISION, and 2K BigGAN images. To make it more challenging, we mix the above 14 testing subsets into another bigger one marked as “Above Mixture” in Table 2, with 28K real and 28K synthetic images. In addition to \mathcal{T}_{open} , we also form a more demanding testing dataset \mathcal{T}_{pra} by collecting images from mainstream sharing platforms. Real-world synthetic images shared and disseminated by users in sharing platforms exhibit much higher quality, compared to randomly generated ones using pre-trained GANs or DMs. Images from \mathcal{T}_{pra} could better reflect practical situations encountered in reality. We gather a total of 4K images from DreamBooth [5], Midjourney [7], NightCafe [8], StableAI [10], and YiJian [12]. Additionally, we obtain 2,229 real painting images drawn by 63 artists from open-source sharing platforms [1, 2]. A preview of these images is available in Fig. 4.

Competitors: The following state-of-the-art synthetic image detectors Wang [76], CR [18], and Grag [40] are selected as comparative methods. Their officially released codes can be obtained from their papers. To ensure the fair comparison, we also *retrain* all the competitors on our training dataset, in addition to directly using their released versions. To make

Table 2. Detection results on open-set \mathcal{T}_{open} by using AUC and Acc as criteria. The best value is **bold**, and the second-best is underlined. †: retrained versions with our training dataset.

Real Dataset	Synthetic Dataset	Wang [76]		Wang† [76]		CR [18]		CR† [18]		Grag [40]		Grag† [40]		Ours		
		AUC	Acc	AUC	Acc	AUC	Acc	AUC	Acc	AUC	Acc	AUC	Acc	AUC	Acc	
ImageNet&VISION	GAN	BigGAN	.6299	.5510	.7456	.7965	.5954	.5525	.7249	.5345	<u>.9000</u>	<u>.9650</u>	.8579	.7955	.9751	.9970
		GauGAN	.8110	.7465	.7935	.6680	.8478	.8185	.8561	.5375	<u>.8983</u>	<u>.9560</u>	.8604	.7995	.9872	.9955
		StyleGAN	.7348	.7108	.8577	.9128	.7432	.7199	.8692	.5584	<u>.9101</u>	<u>.9478</u>	.8983	.7283	.9590	.9850
	DM	DALLE	.5224	.5065	.5160	.5520	.5100	.5110	.5218	.5205	<u>.5954</u>	.5275	.5864	<u>.5605</u>	.7436	.8715
		GLIDE	.5565	.5035	.5740	.5885	.5657	.5000	.6244	.5280	.5745	.5750	<u>.6086</u>	<u>.5995</u>	.8889	.9760
		GuidedDiff	.5117	.5010	<u>.5881</u>	.5770	.5416	.5020	.5840	.5205	.5768	.5210	.5660	<u>.6520</u>	.8769	.9915
	LatentDiff	.5236	.5035	.5930	.6095	.5342	.5045	.5833	.5290	<u>.6491</u>	<u>.6870</u>	.6060	.5065	.8894	.9915	
Artist&Danbooru	GAN	BigGAN	.6519	.5485	<u>.9492</u>	.8830	.6278	.5435	.8920	.9585	.9163	.9585	.9464	<u>.9845</u>	.9887	.9955
		GauGAN	.8299	.7215	<u>.9705</u>	.8990	.8261	.7875	.9350	<u>.9920</u>	.9049	.9435	.9524	.9910	.9889	.9985
		StyleGAN	.7705	.6861	<u>.9789</u>	.9512	.7188	.6928	.9659	<u>.9937</u>	.9138	.9374	.9691	.9725	.9880	.9975
	DM	DALLE	.5365	.5100	.7781	.6165	.5399	.5105	<u>.7823</u>	<u>.8270</u>	.6429	.5250	.7458	.7365	.8842	.9555
		GLIDE	.5379	.5025	<u>.8272</u>	.6680	.5355	.5015	.7543	<u>.8455</u>	.5684	.5535	.7538	.8135	.9720	.9930
		GuidedDiff	.5308	.5025	<u>.8692</u>	.6700	.5155	.5005	.8180	<u>.8970</u>	.5758	.5135	.7164	.6815	.9712	.9930
	LatentDiff	.5369	.5000	<u>.8629</u>	.6755	.5284	.5005	.8442	<u>.9075</u>	.6579	.5950	.7490	.6505	.9750	.9935	
Above Mixture	Above Mixture	.5673	.5804	<u>.7146</u>	.7756	.5563	.5866	.6755	.7690	.6498	.7834	.7065	<u>.8092</u>	.8172	.9466	
Mean		.6168	.5716	<u>.7746</u>	.7229	.6124	.5821	.7621	.7279	.7289	.7326	.7682	<u>.7521</u>	.9270	.9787	

the testing procedures consistent, we select the last layer features of the competitors as their extracted representations.

Evaluation Metrics: Follow the convention [18, 40, 76], we adopt the Area Under the receiver operating characteristic Curve (AUC) and accuracy (Acc) for evaluating the detection performance. Concretely, AUC measures the representation similarity of randomly selected 5K positive and 5K negative sample pairs by using Eq. 4 (with high similarity expected for positive pairs and low for negative ones). Also, Acc is reported to evaluate whether an image in a given test dataset is correctly predicted as either “Real” or “Synthetic”. To predict a hard label “Real” or “Synthetic”, we follow the procedure in Fig. 3 (b), where M real photo (or painting) images randomly picked from ImageNet (or Danbooru) are used as the anchor set. The decision threshold th is set as the median threshold in the AUC metric. Here, we only show the experimental results of $M = 100$, as the value of M just slightly affects the detection performance. More analyses on M is deferred to the appendix.

Implementation Details: We implement our method using the PyTorch deep learning framework, where the Adam [51] with default parameters is adopted as the optimizer. The learning rate is initialized to $1e-4$ and halved if the validation accuracy fails to increase for 2 epochs until the convergence. In the training/testing processes, all the input images are randomly/center cropped into 448×448 patches. Image-domain augmentation, including compression, blurring and scaling, has been applied with 50% probability, which was similarly adopted in [18, 76]. The batch size is set to 48 and the training is performed on 4 NVIDIA A100 GPU 40GB. To facilitate the reproducibility of the results, our code is available at <https://github.com/HighwayWu/LASTED>.

4.2. Evaluation on Open-Set Dataset \mathcal{T}_{open}

The detection results of all competing methods are tabulated in Table 2. It can be seen that the detection performance of Wang [76] and CR [18] is relatively poor, regardless of being retrained or not. Their average Acc values are around 72%, indicating that their models cannot extract discriminative representations in open scenarios. In addition, Grag [40] performs well in distinguishing real photos from GAN synthetic images, which can be reflected by the 96.50% Acc when detecting BigGAN from ImageNet&VISION. However, it still struggles to generalize well to other detection scenarios. For instance, Acc values are only 68.70% when distinguishing LatentDiff from ImageNet&VISION, and 73.65% when classifying DALLE from Artist&Danbooru. In contrast, aided by the language supervision, our proposed LASTED exhibits desirable detection performance in terms of AUC and Acc for all the considered cases. From the results in the last two columns of Table 2, it can be concluded that LASTED possesses excellent generalizability, allowing it to extract highly discriminative representations in multiple cross-domain testing datasets. Overall, our LASTED achieves an average AUC of 92.70% and an average Acc of 97.87%, significantly outperforming the second-ranked competitor by +15.24% and +22.66%, respectively.

4.3. Evaluation on Practical Dataset \mathcal{T}_{pra}

Let us now evaluate the synthetic image detection performance on a more challenging practical dataset \mathcal{T}_{pra} . As can be observed from Table 3, the performance of pre-trained detectors [18, 40, 76] is very poor, with AUC and Acc values close to 50% (random guess). With re-training, they can more effectively grasp the representation of the testing images. For instance, the performance of Grag [40] has increased by +16.50% AUC and +28.81% Acc. Nevertheless,



Figure 4. (a): Each row presents paintings drawn by different artists from [1, 2], and (b) Each row shows DM-generated images from different online platforms [5, 7, 8, 10, 12].

Table 3. Detection results on practical dataset \mathcal{T}_{pra} by using AUC and Acc as criteria. The best value is **bold**, and the second-best is underlined. \dagger : retrained versions with our training dataset.

Real Dataset	Synthetic Dataset	Wang [76]		Wang \dagger [76]		CR [18]		CR \dagger [18]		Grag [40]		Grag \dagger [40]		Ours	
		AUC	Acc	AUC	Acc	AUC	Acc	AUC	Acc	AUC	Acc	AUC	Acc	AUC	Acc
Artist [1, 2]	DreamBooth [5]	.5171	.5001	.6835	.6625	.5204	.5003	.6773	.7747	.5171	.5000	<u>.7155</u>	<u>.8498</u>	.8650	.9183
	MidjourneyV4 [7]	.5243	.5037	.6833	.6972	.5101	.5007	<u>.7013</u>	.7681	.5492	.5022	.6981	<u>.8050</u>	.8286	.8715
	MidjourneyV5 [7]	.5165	.5030	.6602	.6705	.4974	.5015	<u>.6632</u>	.7345	.5091	.5008	.6514	<u>.7395</u>	.7970	.8625
	NightCafe [8]	.5130	.5015	<u>.7926</u>	.7431	.5090	.5038	.7488	.8000	.5342	.5015	.7519	<u>.8215</u>	.8715	.9105
	StableAI [10]	.5067	.5008	<u>.7111</u>	.7349	.5168	.5000	.7015	.7860	.5358	.5302	.7034	<u>.8101</u>	.8083	.8597
	YiJian [12]	.5362	.5023	.5980	.5427	.5422	.5113	.5876	.5992	.5420	.5025	<u>.6568</u>	<u>.7399</u>	.7462	.8103
Mean		.5190	.5019	.6881	.6752	.5160	.5029	.6800	.7438	.5312	.5062	<u>.6962</u>	<u>.7943</u>	.8194	.8721

the classification-based training paradigm still limits the generalization of the learned image representations, leading to inferior detection performance. In contrast, our language-guided contrastive learning paradigm empowers the model to learn more generalizable image representations, achieving an average of 81.94% AUC and 87.21% Acc, which outperform the second place by +12.32% and +7.78%, respectively.

In addition to experiments on \mathcal{T}_{open} and \mathcal{T}_{pra} , we also evaluate the performance of LASTED and competitors on the ForenSynths dataset proposed in [76], which is primarily composed of GAN images (and hence relatively less challenging). Again, our LASTED outperforms the other methods by a big margin. Detailed experimental settings and results can be found in the appendix.

4.4. Ablation Studies

In this subsection, we conduct the ablation studies of LASTED by analyzing how the training paradigm, language supervision, and network architecture contribute to the eventual detection performance. The comparative results are given in Table 4, which, due to page limit, only includes a part of testing datasets from \mathcal{T}_{open} .

Training Paradigm In Table 4, the results of LASTED are given in row #5. We also train the same network using a standard classification and contrastive paradigm, and the results are reported in rows #1~#4. More specifically, we add a fully connected layer to implement the classification-based framework, while in the standard contrastive paradigm,

we use the cyclic loss [73] to supervise the image encoder, without involving any text encoder. It is obvious that the classification paradigm (either 2-class or 4-class) is not sufficient to extract generalizable representations, achieving only 80.74% Acc at most. The networks trained with the standard (image-level) contrastive paradigm achieve slightly better generalization, with 83.56% Acc. It should be emphasized that the objective function of the standard contrastive paradigm is much more difficult to be optimized, making the model easily get trapped in local optima. Also, it does not consider the relationship among different categories. Our proposed LASTED, with the help of language-guided contrastive paradigm, can better address the above issues, greatly enhancing the model’s generalizability with 95.12% Acc.

Language Label Representation As mentioned in Sec. 3.2, language supervision has various textual labeling strategies that could affect the detection performance. In rows #5~#8, we compare four labeling choices. Specifically, row #6 explicitly breaks the connection among different categories using hyphens; namely, the implicit relationship between “Real-Photo” and “Real-Painting” categories (similarly for other cases) conveyed by the word “Real” is lost. In this case, we observe a 6.12% performance drop, compared to row #5, implying that the ability to learn shared representations of different “Real” images is weakened. Unsurprisingly, if we use labels “Real” and “Synthetic” only, the model’s performance is significantly degraded. It is because the naive labeling forces the model to learn common

Table 4. Ablation studies regarding the training paradigm, architecture, and label representation. Acc is adopted as the criterion. Here, IV, AD, and AM are abbreviations for ImageNet&VISION, Artist&Danbooru, and “Above Mixture”, respectively.

#	Training Paradigm	Architecture	Label Representation	Testing Datasets (Real / Synthetic)					Mean	
				IV/StyleGAN	IV/DALLE	AD/StyleGAN	AD/DALLE	AM/AM		
#1	Classification	RN50x64	0, 1, 2, 3	.8264	.7425	.8310	.7440	.8932	.8074	
#2			0, 1	.7629	.6890	.8146	.7430	.7866	.7592	
#3	Contrastive (w/o LASTED)	RN50x64	0, 1, 2, 3	.8197	.7395	.9750	.7460	.8976	.8356	
#4			0, 1	.7890	.6625	.9545	.7620	.7342	.7804	
#5	Contrastive (w LASTED)	RN50x64	\mathcal{R}_2 in Table 1	.9850	.8715	.9975	.9555	.9466	.9512	
#6			\mathcal{R}_4 in Table 1	.9787	.7905	.9958	.7670	.9180	.8900	
#7			\mathcal{R}_1 in Table 1	.9230	.7495	.9879	.7330	.7942	.8375	
#8			\mathcal{R}_5 in Table 1	.9846	.8713	.9983	.9550	.9463	.9511	
#9			RN50	\mathcal{R}_2 in Table 1	.9265	.7795	.9904	.9235	.8728	.8985
#10			ViT-L	\mathcal{R}_2 in Table 1	.8301	.7205	.9412	.8220	.6864	.8000

representations from different types of image (e.g., “Photo” and “Painting”), which is not conducive to optimization. Such a phenomenon can also be noticed in the classification paradigm and standard contrastive paradigm, such as row #2 compared to row #1, and row #4 compared to row #3, which respectively have 4.82% to 5.52% performance drop. Interestingly, the results of rows #8 and #5 are almost identical, indicating that the specific words such as “Real”, “Synthetic”, “Photo” or “Painting” are not important, as long as the relationship among textual labels preserves.

Network Architecture Different network architectures inherently possess varying representation abilities. We now evaluate the detection performance when ResNet50 [45], ResNet50x64 [65], ConvNeXt [55], ViT [52], and MiT [78] are used. Specifically, the results for ResNet50x64, ResNet50, and ViT-L can be found in rows #5, #9, and #10 of Table 4, respectively. As can be noticed, for the task of synthetic image detection, ResNet-based networks are more suitable than Transformers. As a result, we ultimately select ResNet50x64 as our network architecture.

4.5. Robustness to Post-processing

We also analyze the robustness of all competing detectors against post-processing operations. This is crucial because the given images under investigation may have gone through various post-processing operations. To this end, we select four commonly-used operations, including JPEG compression, Gaussian blurring, Gaussian noise, and down-sampling. We then apply them to the challenging practical dataset \mathcal{T}_{pra} , and show the results in Fig. 5. It can be seen that CR [18] and Grag [40] are somewhat vulnerable against JPEG compression, especially when the quality factors (QFs) are small. For instance, when QF is 50, the performance drop can be more than 10%. Fortunately, our LASTED consistently demonstrates satisfactory robustness against these post-processing interference.

5. Conclusions

This paper addresses an important issue on how to improve the generalization of synthetic image detector. To this end, we propose LASTED, a language-guided contrastive

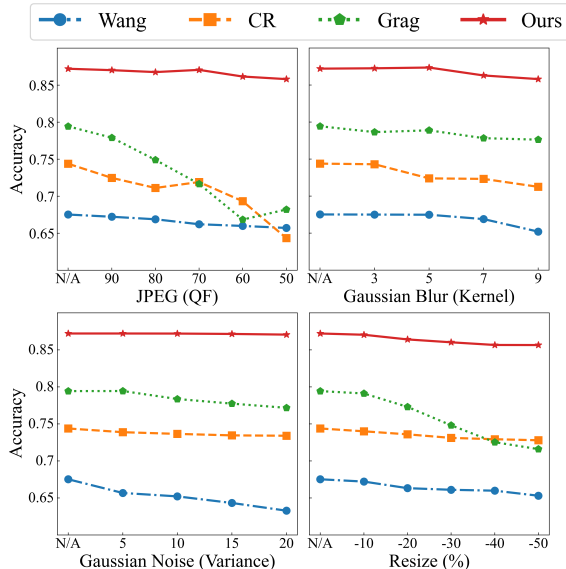


Figure 5. Robustness evaluations against compression, blurring, noise addition, and resizing.

learning framework with novel training paradigm and testing procedure, for the generalizable synthetic image detection. Extensive experiments are provided to demonstrate the strong generalizability of our proposed LASTED, which outperforms the state-of-the-art competitors by a big margin.

Appendix A. Effect of Anchor Set Size M

To investigate the appropriate size of the anchor set in the synthetic image detection task, we conduct comparative experiments on the testing set \mathcal{T}_{open} using different values of M : 1, 10, 50, 100, 200 to 500. For each value of M , we run 50 independent experiments, and present the mean and standard deviation of the results in Fig 6. It can be observed that when $M = 1$, the performance is highly unstable, with a very big standard deviation being 0.14. As M increases, the AUC performance gradually stabilizes, primarily because the averaged feature of the anchor set better represents the “ground-truth” of the anchor category. Considering the cost of acquiring anchor data and the ultimate performance, we set $M = 100$ in our experiments.

Table 5. Detection results on ForenSynths dataset [76] by using AP as a criterion. For each column, the best value is **bold**, and the second-best is underlined. Noted that all the methods are trained on the ProGAN subset while being tested for generalization on the remaining 10 subsets. Wang-0.1 and Wang-0.5 represent two variants trained with 10% and 50% data augmentation, respectively.

Methods	Subsets of ForenSynths [76]									Mean	
	StyleGAN	BigGAN	CycleGAN	StarGAN	GauGAN	CRN	IMLE	SITD	SAN		Deepfake
Wang-0.5 [76]	.985	.882	.968	.954	.981	.989	.995	.927	.639	.663	.898
Wang-0.1 [76]	<u>.996</u>	.845	.935	.982	.895	.982	.984	<u>.972</u>	<u>.705</u>	.890	<u>.919</u>
Grag [40]	.963	<u>.891</u>	.924	<u>.988</u>	.912	.927	.927	.764	.520	.519	.834
CR [18]	.986	.881	.957	.939	<u>.990</u>	<u>.993</u>	<u>.998</u>	.799	.657	.716	.892
Ours	.998	.992	.978	.999	.991	.998	.999	.997	.929	<u>.865</u>	.975

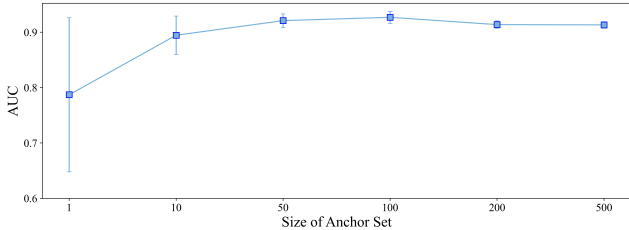


Figure 6. The impact of the anchor set size M on the detection performance over the testing set \mathcal{T}_{open} .

Appendix B. Further Evaluation on ForenSynths Dataset [76]

In addition to the experiments on the open-set dataset \mathcal{T}_{open} and the practical dataset \mathcal{T}_{pra} , we also evaluate the performance of our LASTED and other competing methods on the ForenSynths [76] dataset, which is primarily composed of GAN-generated images (and hence relatively less challenging). To be fair enough, we strictly follow the experimental settings and testing procedures in Wang [76]. More specifically, the ForenSynths dataset is comprised of 11 subsets generated by 11 synthetic approaches, including ProGAN [49], StyleGAN [50], BigGAN [15], CycleGAN [83], StarGAN [21], GauGAN [63], CRN [20], IMLE [53], SITD [19], SAN [26], and Deepfake [4]. To assess how well the synthetic image detectors generalize to unseen images, only the ProGAN subset is utilized for the training, while the remaining 10 subsets are used for the testing. Since ProGAN only consists of “Photo” signals, we adopt \mathcal{R}_1 as text labels in LASTED. Again, to be consistent with the setting in [76], we use the average precision (AP) as the evaluation metric.

The comparative results are presented in Table 5. In general, all considered methods exhibit desirable generalization capabilities to other GAN-generated images, achieving high detection precision (over 90% AP) on subsets StyleGAN, CycleGAN, StarGAN, and GauGAN. This phenomenon is not surprising, as many different GANs and GAN-like generative models tend to leave similar traces. However, the detection performance of the existing methods on SAN and Deepfake becomes much inferior, demonstrating their inadequate generalizability. As can be seen in the last row of

Table 5, our LASTED offers satisfactory detection performance for all the 10 testing cases, with average AP being 97.5%. This again validates that our LASTED could learn more generalizable representations for the synthetic image detection.

Appendix C. More Discussions on Related Works

In addition to the related works introduced in the main file, very recently (some are several days before the submission deadline), many studies [13, 14, 16, 22, 31, 32, 36, 41, 42, 54, 62, 64, 68, 72, 74, 75, 77] have been conducted for detecting GAN- or DM-generated images. Specifically, [22, 32, 54, 68, 74] facilitated the extraction of synthetic artifacts by introducing frequency-aware attentional feature or learnable noise pattern (LNP) in amplitude and phase spectra domains. Due to the vulnerability of frequency-domain features in synthetic images, these methods are not robust against various inferences [32]. In addition, Wang *et al.* [77] discovered that the features of DM-generated images are more easily reconstructed by pre-trained DM models, compared to real ones. They then defined the Diffusion Reconstruction Error (DIRE), based on which DM-generated and real images can be distinguished. Nevertheless, DIRE has only been validated in rather constrained scenarios (specifically, bedroom images synthesized by DMs), and the extension to more general cases is unclear. Amoroso *et al.* [13] proposed the decoupling of semantic and style features of images, showing that synthetic images may be more easily separable in the style domain. However, the applicability of semantic-style disentangling is limited, as it requires training sets that encompass data with the same style but different semantics, or data with the same semantics but different styles. By utilizing meticulously designed training sets, Guo *et al.* [42] and Guarnera *et al.* [41] defined hierarchical fine-grained labels for forged or synthetic images, enabling the detector to learn not only comprehensive features but also the inherent hierarchical nature of different attributes. Unfortunately, the hierarchical formulation necessitates the inclusion of too many forgery techniques in the training set. This may pose challenges when applied to situations with limited training set diversity. Considering the difficulties of applying a detec-

tor to detect unknown types of image, some other approaches suggested enhancing the detector’s generalization capability through model transferability [72], data adaptability [62], or data augmentation [31], etc.

It should be emphasized, from the perspective of comparative studies, that the codes and pre-trained weights of these very recent methods have NOT been made publicly available so far. As a result, we have not yet included their comparative analyses into the current work.

Appendix D. Broader Impacts

The proliferation of AI-generated content (AIGC) has led to significant concerns about the authenticity of images from various communities. It is therefore crucial to develop effective detectors with high detection capabilities to tell AIGC images from real ones. Furthermore, the rapid evolution of deep learning has resulted in a constant stream of AIGC models, posing even greater challenges to the generalization ability of detectors. The LASTED method proposed in this paper, with its exceptional detection performance and generalization ability, could serve as a valuable asset for the forensic community in the task of synthetic image detection.

Appendix E. Limitations

Although our proposed LASTED performs well in the experiments, it still has room for further improvements. Due to the limited training dataset, which mainly includes photos and paintings, LASTED may suffer from a performance decline in extracting highly generalizable forensic features from some unseen image types, such as medical images or satellite images. Such a limitation could be alleviated by introducing more image categories into the training phase. Additionally, incorporating domain generalization techniques (e.g., [82]), could further improve the generalizability of the LASTED to combat unseen GAN- or DM-synthesized images.

References

- [1] Artstation: Showcase platform for art and design. <https://www.artstation.com/>.
- [2] Behance: A platform for creative professionals. <https://www.behance.net/>.
- [3] Danbooru2021: A large-scale crowdsourced and tagged anime illustration dataset. <https://www.gwern.net/Danbooru2021>.
- [4] Deepfakes github. <https://github.com/deepfakes/faceswap>.
- [5] Dreambooth: Tailor-made ai image generation. <https://www.strmr.com/>.
- [6] Lexica: A stable diffusion search engine. <https://lexica.art/>.
- [7] Midjourney: Expanding the imaginative powers. <https://midjourney.com/>.
- [8] Nightcafe: Create amazing artworks using the power of artificial intelligence. <https://creator.nightcafe.studio/>.
- [9] Novelai: Ai-assisted authorship, storytelling, and virtual companionship. <https://novelai.net/>.
- [10] Stability.ai: Stable diffusion public release. <https://stability.ai/blog/stable-diffusion-public-release>.
- [11] Stable-diffusion-v1-5. <https://huggingface.co/runwayml/stable-diffusion-v1-5>.
- [12] Yijian: Chinese ai painting creative cloud. <https://creator.nightcafe.studio/>.
- [13] R. Amoroso, D. Morelli, M. Cornia, L. Baraldi, A. Del Bimbo, and R. Cucchiara. Parents and children: Distinguishing multimodal deepfakes from natural images. *arXiv preprint arXiv:2304.00500*, 2023.
- [14] J. Bird and A. Lotfi. Cifake: Image classification and explainable identification of ai-generated synthetic images. *arXiv preprint arXiv:2303.14126*, 2023.
- [15] A. Brock, J. Donahue, and K. Simonyan. Large scale gan training for high fidelity natural image synthesis. In *Proc. Int. Conf. Learn. Representat.*, pages 1–35, 2018.
- [16] T. Bui, N. Yu, and J. Collomosse. Repmix: Representation mixing for robust attribution of synthesized images. In *Proc. IEEE Conf. Comput. Vis. Pattern Recogn.*, pages 146–163, 2022.
- [17] L. Chai, D. Bau, S. Lim, and P. Isola. What makes fake images detectable? understanding properties that generalize. In *Proc. Eur. Conf. Comput. Vis.*, pages 103–120, 2020.
- [18] K. Chandrasegaran, N. T. Tran, A. Binder, and N. M. Cheung. Discovering transferable forensic features for cnn-generated images detection. In *Proc. Eur. Conf. Comput. Vis.*, pages 671–689, 2022.
- [19] C. Chen, Q. Chen, J. Xu, and V. Koltun. Learning to see in the dark. In *Proc. IEEE Conf. Comput. Vis. Pattern Recogn.*, pages 3291–3300, 2018.
- [20] Q. Chen and V. Koltun. Photographic image synthesis with cascaded refinement networks. In *Proc. IEEE Int. Conf. Comput. Vis.*, pages 1511–1520, 2017.
- [21] Y. Choi, M. Choi, M. Kim, J. Ha, S. Kim, and J. Choo. Stargan: Unified generative adversarial networks for multi-domain image-to-image translation. In *Proc. IEEE Conf. Comput. Vis. Pattern Recogn.*, pages 8789–8797, 2018.
- [22] R. Corvi, D. Cozzolino, G. Poggi, K. Nagano, and L. Verdoliva. Intriguing properties of synthetic images: from generative adversarial networks to diffusion models. *arXiv preprint arXiv:2304.06408*, 2023.
- [23] R. Corvi, D. Cozzolino, G. Zingarini, G. Poggi, K. Nagano, and L. Verdoliva. On the detection of synthetic images generated by diffusion models. In *Proc. IEEE Int. Conf. Acoust. Speech Signal Process.*, pages 1–5, 2023.
- [24] D. Cozzolino, D. Gragnaniello, G. Poggi, and L. Verdoliva. Towards universal gan image detection. In *Inter. Conf. on Vis. Commu. and Image Proc.*, pages 1–5, 2021.
- [25] D. Cozzolino and L. Verdoliva. Noiseprint: a cnn-based camera model fingerprint. *IEEE Trans. Inf. Forensics Secur.*, 15(1):114–159, 2020.

- [26] T. Dai, J. Cai, Y. Zhang, S. Xia, and L. Zhang. Second-order attention network for single image super-resolution. In *Proc. IEEE Conf. Comput. Vis. Pattern Recogn.*, pages 11065–11074, 2019.
- [27] J. Deng, W. Dong, R. Socher, L. J. Li, K. Li, and F. Li. Imagenet: a large-scale hierarchical image database. In *Proc. IEEE Conf. Comput. Vis. Pattern Recogn.*, pages 248–255, 2009.
- [28] J. Deng, J. Guo, N. Xue, and S. Zafeiriou. Arcface: Additive angular margin loss for deep face recognition. In *Proc. IEEE Conf. Comput. Vis. Pattern Recogn.*, pages 4690–4699, 2019.
- [29] L. Van der Maaten and G. Hinton. Visualizing data using t-sne. *Journal of Mach. Learn. Res.*, 9(11), 2008.
- [30] P. Dhariwal and A. Nichol. Diffusion models beat gans on image synthesis. volume 34, pages 8780–8794, 2021.
- [31] P. Dogoulis, G. Kordopatis-Zilos, I. Kompatsiaris, and S. Papadopoulos. Improving synthetically generated image detection in cross-concept settings. *arXiv preprint arXiv:2304.12053*, 2023.
- [32] C. Dong, A. Kumar, and E. Liu. Think twice before detecting gan-generated fake images from their spectral domain imprints. In *Proc. IEEE Conf. Comput. Vis. Pattern Recogn.*, pages 7865–7874, 2022.
- [33] R. Durall, M. Keuper, and J. Keuper. Watch your up-convolution: Cnn based generative deep neural networks are failing to reproduce spectral distributions. In *Proc. IEEE Conf. Comput. Vis. Pattern Recogn.*, pages 7890–7899, 2020.
- [34] T. Dzanic, K. Shah, and F. Witherden. Fourier spectrum discrepancies in deep network generated images. *Proc. Adv. Neural Inf. Process. Syst.*, 33:3022–3032, 2020.
- [35] R. Feng, D. Zhao, and Z. Zha. Understanding noise injection in gans. In *Proc. Int. Conf. Mach. Learn.*, pages 3284–3293, 2021.
- [36] A. Ferreira, E. Nowroozi, and M. Barni. Vipprint: Validating synthetic image detection and source linking methods on a large scale dataset of printed documents. *Journal of Imaging*, 7(3):50–73, 2021.
- [37] J. Frank, T. Eisenhofer, L. Schonherr, A. Fischer, D. Kolossa, and T. Holz. Leveraging frequency analysis for deep fake image recognition. In *Proc. Int. Conf. Mach. Learn.*, pages 3247–3258, 2020.
- [38] S. Girish, S. Suri, S. Rambhatla, and A. Shrivastava. Towards discovery and attribution of open-world gan generated images. In *Proc. IEEE Int. Conf. Comput. Vis.*, pages 14094–14103, 2021.
- [39] O. Giudice, L. Guarnera, and S. Battiato. Fighting deepfakes by detecting gan dct anomalies. *J. of Imaging*, 7(8):128, 2021.
- [40] D. Gragnaniello, D. Cozzolino, F. Marra, G. Poggi, and L. Verdoliva. Are gan generated images easy to detect? a critical analysis of the state-of-the-art. In *Proc. IEEE Inter. Conf. Multimed. Expo*, pages 1–6, 2021.
- [41] L. Guarnera, O. Giudice, and S. Battiato. Level up the deepfake detection: a method to effectively discriminate images generated by gan architectures and diffusion models. *arXiv preprint arXiv:2303.00608*, 2023.
- [42] X. Guo, X. Liu, Z. Ren, S. Grosz, I. Masi, and X. Liu. Hierarchical fine-grained image forgery detection and localization. *arXiv preprint arXiv:2303.17111*, 2023.
- [43] K. He, X. Chen, S. Xie, Y. Li, P. Dollár, and R. Girshick. Masked autoencoders are scalable vision learners. In *Proc. IEEE Conf. Comput. Vis. Pattern Recogn.*, pages 16000–16009, 2022.
- [44] K. He, H. Fan, Y. Wu, S. Xie, and R. Girshick. Momentum contrast for unsupervised visual representation learning. In *Proc. IEEE Conf. Comput. Vis. Pattern Recogn.*, pages 9729–9738, 2020.
- [45] K. He, X. Zhang, S. Ren, and J. Sun. Deep residual learning for image recognition. In *Proc. IEEE Conf. Comput. Vis. Pattern Recogn.*, pages 770–778, 2016.
- [46] Y. He, N. Yu, M. Keuper, and M. Fritz. Beyond the spectrum: Detecting deepfakes via re-synthesis. In *Proc. Inter. Joint Conf. on Arti. Intell.*, pages 2534–2541, 2021.
- [47] Y. Jeong, D. Kim, Y. Ro, P. Kim, and J. Choi. Fingerprintnet: Synthesized fingerprints for generated image detection. In *Proc. Eur. Conf. Comput. Vis.*, pages 76–94, 2022.
- [48] Y. Ju, S. Jia, L. Ke, H. Xue, K. Nagano, and S. Lyu. Fusing global and local features for generalized ai-synthesized image detection. In *Proc. IEEE Int. Conf. on Im. Proc.*, pages 3465–3469, 2022.
- [49] T. Karras, T. Aila, S. Laine, and J. Lehtinen. Progressive growing of gans for improved quality, stability, and variation. In *Proc. Int. Conf. Learn. Representat.*, 2018.
- [50] T. Karras, S. Laine, and T. Aila. A style-based generator architecture for generative adversarial networks. In *Proc. IEEE Conf. Comput. Vis. Pattern Recogn.*, pages 4401–4410, 2019.
- [51] D. P. Kingma and J. Ba. Adam: a method for stochastic optimization. *arXiv preprint arXiv:1412.6980*, 2014.
- [52] A. Kolesnikov, A. Dosovitskiy, D. Weissenborn, G. Heigold, J. Uszkoreit, L. Beyer, M. Minderer, M. Dehghani, N. Houlsby, S. Gelly, T. Unterthiner, and X. Zhai. An image is worth 16x16 words: Transformers for image recognition at scale. In *Proc. Int. Conf. Learn. Representat.*, pages 1–22, 2021.
- [53] K. Li, T. Zhang, and J. Malik. Diverse image synthesis from semantic layouts via conditional imle. In *Proc. IEEE Int. Conf. Comput. Vis.*, pages 4220–4229, 2019.
- [54] B. Liu, F. Yang, X. Bi, B. Xiao, W. Li, and X. Gao. Detecting generated images by real images. In *Proc. Eur. Conf. Comput. Vis.*, pages 95–110, 2022.
- [55] Z. Liu, H. Mao, C. Wu, C. Feichtenhofer, T. Darrell, and S. Xie. A convnet for the 2020s. In *Proc. IEEE Conf. Comput. Vis. Pattern Recogn.*, pages 11976–11986, 2022.
- [56] S. Mandelli, D. Cozzolino, P. Bestagini, L. Verdoliva, and S. Tubaro. Cnn-based fast source device identification. *IEEE Signal. Proc. Let.*, 27(1):1285–1289, 2020.
- [57] F. Marra, C. Saltori, G. Boato, and L. Verdoliva. Incremental learning for the detection and classification of gan-generated images. In *Proc. IEEE Int. Workshop Inf. Forensics Secur.*, pages 1–6, 2019.
- [58] O. Mayer and M. C. Stamm. Forensic similarity for digital images. *IEEE Trans. Inf. Forensics Secur.*, 15(1):1331–1346, 2020.
- [59] Q. Meng, S. Zhao, Z. Huang, and F. Zhou. Magface: A universal representation for face recognition and quality assessment. In *Proc. IEEE Conf. Comput. Vis. Pattern Recogn.*, pages 14225–14234, 2021.

- [60] A. Nichol, P. Dhariwal, A. Ramesh, P. Shyam, P. Mishkin, B. McGrew, I. Sutskever, and M. Chen. Glide: Towards photorealistic image generation and editing with text-guided diffusion models. In *Proc. Int. Conf. Mach. Learn.*, pages 16784–16804, 2022.
- [61] A. Odena, V. Dumoulin, and C. Olah. Deconvolution and checkerboard artifacts. *Distill*, 1(10):e3, 2016.
- [62] U. Ojha, Y. Li, and Y. Lee. Towards universal fake image detectors that generalize across generative models. *arXiv preprint arXiv:2302.10174*, 2023.
- [63] T. Park, M. Liu, T. Wang, and J. Zhu. Semantic image synthesis with spatially-adaptive normalization. In *Proc. IEEE Conf. Comput. Vis. Pattern Recogn.*, pages 2337–2346, 2019.
- [64] T. Qiao, Y. Chen, X. Zhou, R. Shi, H. Shao, K. Shen, and X. Luo. Csc-net: Cross-color spatial co-occurrence matrix network for detecting synthesized fake images. *IEEE Trans. on Cogni. and Devel.l Syst.*, pages 1–11, 2023.
- [65] A. Radford, J. Kim, C. Hallacy, A. Ramesh, G. Goh, S. Agarwal, G. Sastry, A. Askell, P. Mishkin, J. Clark, K. Gretchen, and S. Ilya. Learning transferable visual models from natural language supervision. In *Proc. Int. Conf. Mach. Learn.*, pages 8748–8763, 2021.
- [66] A. Radford, J. Wu, R. Child, D. Luan, D. Amodei, and I. Sutskever. Language models are unsupervised multitask learners. *OpenAI blog*, 1(8):9, 2019.
- [67] A. Ramesh, P. Dhariwal, A. Nichol, C. Chu, and M. Chen. Hierarchical text-conditional image generation with clip latents. *preprint arXiv:2204.06125*, 2022.
- [68] J. Ricker, S. Damm, T. Holz, and A. Fischer. Towards the detection of diffusion model deepfakes. *arXiv preprint arXiv:2210.14571*, 2022.
- [69] R. Rombach, A. Blattmann, D. Lorenz, P. Esser, and B. Ommer. High-resolution image synthesis with latent diffusion models. In *Proc. IEEE Conf. Comput. Vis. Pattern Recogn.*, pages 10684–10695, 2022.
- [70] Z. Sha, Z. Li, N. Yu, and Y. Zhang. De-fake: Detection and attribution of fake images generated by text-to-image diffusion models. *preprint arXiv:2210.06998*, 2022.
- [71] D. Shullani, M. Fontani, M. Iuliani, O. Shaya, and A. Piva. Vision: a video and image dataset for source identification. *EURASIP J. on Info. Security*, 15(1):1–16, 2017.
- [72] S. Sinitza and O. Fried. Deep image fingerprint: Accurate and low budget synthetic image detector. *arXiv preprint arXiv:2303.10762*, 2023.
- [73] Y. Sun, C. Cheng, Y. Zhang, C. Zhang, L. Zheng, Z. Wang, and Y. Wei. Circle loss: A unified perspective of pair similarity optimization. In *Proc. IEEE Conf. Comput. Vis. Pattern Recogn.*, pages 6398–6407, 2020.
- [74] C. Tian, Z. Luo, G. Shi, and S.Li. Frequency-aware attentional feature fusion for deepfake detection. In *Proc. IEEE Int. Conf. Acoust. Speech Signal Process.*, pages 1–5, 2023.
- [75] H. Wang, J. Fei, Y. Dai, L. Leng, and Z. Xia. General gan-generated image detection by data augmentation in fingerprint domain. *arXiv preprint arXiv:2212.13466*, 2022.
- [76] S. Wang, O. Wang, R. Zhang, A. Owens, and A. A. Efros. Cnn-generated images are surprisingly easy to spot... for now. In *Proc. IEEE Conf. Comput. Vis. Pattern Recogn.*, pages 8695–8704, 2020.
- [77] Z. Wang, J. Bao, W. Zhou, W. Wang, H. Hu, H. Chen, and H. Li. Dire for diffusion-generated image detection. *arXiv preprint arXiv:2303.09295*, 2023.
- [78] E. Xie, W. Wang, Z. Yu, A. Anandkumar, J. Alvarez, and P. Luo. Segformer: Simple and efficient design for semantic segmentation with transformers. In *Proc. Neural Info. Process. Syst.*, pages 12077–12090, 2021.
- [79] F. Yu, A. Seff, Y. Zhang, S. Song, T. Funkhouser, and J. Xiao. Lsun: Construction of a large-scale image dataset using deep learning with humans in the loop. *preprint arXiv:1506.03365*, 2015.
- [80] M. Zhang, H. Wang, P. He, A. Malik, and H. Liu. Improving gan-generated image detection generalization using unsupervised domain adaptation. In *Proc. IEEE Inter. Conf. Multim. Expo*, pages 1–6, 2022.
- [81] X. Zhang, S. Karaman, and S. Chang. Detecting and simulating artifacts in gan fake images. In *Proc. IEEE Int. Workshop Inf. Forensics Secur.*, pages 1–6, 2019.
- [82] K. Zhou, Z. Liu, Y. Qiao, T. Xiang, and C. Loy. Domain generalization: A survey. *IEEE Trans. Pattern Anal. and Mach. Intell.*, 45(4):4396–4415, 2023.
- [83] J. Zhu, T. Park, P. Isola, and A. Efros. Unpaired image-to-image translation using cycle-consistent adversarial networks. In *Proc. IEEE Int. Conf. Comput. Vis.*, pages 2223–2232, 2017.